Bistability of an HIV Model with Immune Impairment*

Shaoli Wang[†], Tengfei Wang[†], Fei Xu[‡], and Libin Rong[§]

Abstract. The immune response is a crucial factor in controlling HIV infection. However, oxidative stress poses a significant challenge to the HIV-specific immune response, compromising the body's ability to control viral replication. In this paper, we develop an HIV infection model to investigate the impact of immune impairment on virus dynamics. We derive the basic reproduction number (R_0) and threshold (R_c) . Utilizing the antioxidant parameter as a bifurcation parameter, we establish that the system exhibits saddle-node bifurcation backward and forward bifurcations. Specifically, when $R_0 > R_c$, the virus will rebound if the antioxidant parameter falls below the post-treatment control threshold. Conversely, when the antioxidant parameter exceeds the elite control threshold, the virus remains under elite control. The region between the two thresholds represents a bistable interval. These results can explain why some HIV-infected patients experience rapid viral rebound after treatment cessation while others achieve post-treatment control for a longer time.

Key words. immune impairment, post-treatment control threshold, elite control threshold, saddle-node bifurcation, backward bifurcation

MSC codes. 34D20, 92B05

DOI. 10.1137/23M1596004

1. Introduction. HIV mainly infects activated CD4⁺ T cells. During the early stage of HIV infection, the virus significantly decreases the number of CD4⁺ T cells. The host initially responds rapidly and nonspecifically by activating natural killer cells, macrophages, and other innate immune responses. Then, the level of CD4⁺ T cells remains almost constant or very slowly declines for several years due to the viral inhibition provided by the adaptive immune response. The host develops virus-specific adaptive responses by activating cytotoxic T lymphocytes (CTLs) and antibody-producing cells. CTLs attack infected cells while antibodies target the viruses, providing an antiviral defense for the host.

The dynamics of viral infection and the immune responses have been investigated using mathematical models. For example, the references [13, 25] used a model to study the interplay between activated CD4⁺ T cells, infected CD4⁺ T cells, viruses, and immune cells.

^{*}Received by the editors August 23, 2023; accepted for publication (in revised form) by K. Tsaneva-Atanasova January 8, 2024; published electronically May 2, 2024.

https://doi.org/10.1137/23M1596004

Funding: The work of the first author was supported by the National Natural Science Foundation of China (U21A20206), Scientific and Technological Research Projects of Henan Province (242102310229) and Natural Science Foundations of Henan (192102310089, 202300410045). The work of the fourth author was supported by the NSF grants DMS-1950254 and DMS-2324692.

[†]School of Mathematics and Statistics, Henan University, Kaifeng, 475001, People's Republic of China (wslheda@163.com, wangtf1999@foxmail.com).

[‡]Department of Mathematics, Wilfrid Laurier University, Waterloo, N2L 3C5, Canada (fxu.feixu@gmail.com).

[§]Department of Mathematics, University of Florida, Gainesville, FL 32611 USA (libinrong@ufl.edu).

Komarova et al. [22] modeled the interrelationship among timing and efficiency of antiviral drug therapy. References [1] and [40] studied HIV infection and showed that the turnover rate of free virus is much faster than that of infected cells. Based on these findings, they used the quasi-steady-state assumption, which means that the viral load is proportional to the number of infected cells. As a result, the dimension of the model can be reduced, facilitating the parameter estimation using available viral load data. Models have also been developed to explore the spread of HIV infection, taking into account factors such as mobility [41] and transmission among MSM (men who have sex with men) [44].

HIV can mutate into new forms that escape specific immune responses. Because of prolonged exposure to the virus, chronic inflammation, and the release of inhibitory molecules by the virus, immune exhaustion also occurs and T cells become less responsive and effective in their ability to kill virus-infected cells; see [5, 11, 18, 19, 20, 26, 28, 29]. Regoes, Wodarz, and Nowak, [31] performed investigations on a variety of HIV models with immune impairment. They showed that when the impairment rate overwhelms a threshold value, the immune system of the host may collapse. Iwami and his colleagues [16, 17] constructed mathematical models to study HIV infection and carried out an analysis to obtain a "risky threshold" and an "immunodeficiency threshold" for the impairment rate. Their investigations imply that when the impairment rate is greater than the threshold value, the immune system of the host always collapses.

Combination antiretroviral therapy (ART) can suppress HIV for long periods, keeping the virus undetectable. However, the therapy cannot eradicate the virus. The latent HIV reservoir consisting of latently infected CD4+ T cells can be established very rapidly after the infection. These latent cells can survive ART and remain unaffected by the immune response. They can be activated to produce new virus, igniting new infections. When patients stop the ART, the plasma viremia can rebound to a detectable level. Thus, the latent reservoir represents a major barrier to the elimination of HIV. Mathematical models have been employed to investigate HIV treatment. For instance, in [24], the authors devised an optimal treatment strategy for combined ART. This strategy aims to maximize the levels of healthy CD4⁺ T cells while minimizing side effects and costs. The dynamics of the latent reservoir have also been investigated [21, 33, 34, 37]. In [37], the authors investigated HIV infection with the latent reservoir activation using a stochastic simulation. They showed that the latent reservoir has a relatively stable size. In [21], the influence of ongoing viral replication on the evolution of the latent reservoir was investigated, and the authors revealed the influences of a variety of viral and host factors on the dynamics of the latent reservoirs. In [33], a mathematical model was established to study the activation of latently infected cells, and the mechanism behind the replenishment of latent reservoirs was investigated.

The time to viral rebound after treatment termination is of great interest. Many patients experienced viral rebound to a detectable level within a couple of weeks. However, the case of the "Mississippi baby" is different. The infant was started on ART within 30 hours of birth, much earlier than the standard practice of initiating ART in HIV-exposed infants at 4–6 weeks of age. The baby's viral load became undetectable after several weeks of treatment, and the infant remained on ART for approximately 18 months. In 2013, at 30 months of age, the baby was reported as a potential cure for HIV, as the baby's viral load remained undetectable 12 months after ART was discontinued. However, in 2014 when the child was 46 months

old, it was announced that the virus had rebounded in the child's blood, and the functional cure was no longer considered to be achieved. Despite the outcome of the Mississippi baby case, it has provided valuable insights into the potential for early and aggressive treatment of HIV-infected patients [27].

Conway and Perelson [7] developed a mathematical model to study the viral rebound after treatment interruption. They predicted that the strength of the immune response and the initial size of the latent reservoir could affect the dynamics. Their results suggest that patients who receive ART early after HIV infection have a higher chance of achieving post-treatment control, where the amount of plasma virus remains undetectable after the termination of medical treatment. However, only a small proportion of such patients attain post-treatment control. Further investigations are needed to reveal the mechanism behind post-treatment control.

Oxidative stress refers to an imbalance between the production of reactive oxygen species (ROS), which are highly reactive molecules, and the ability of cells to detoxify and repair the resulting damage [8]. Oxidative stress can have multiple detrimental effects on HIV infection and immune response [35], including promoting viral replication [14, 43], impairing immune cell function [12, 36, 43], triggering inflammation [32], and depleting antioxidant defenses [15]. Managing oxidative stress may be an important therapeutic strategy in the management of HIV infection to potentially reduce disease progression and improve immune function. In this paper, we develop a mathematical model to better understand the complex interplay between oxidative stress and HIV infection. The model is given by

(1.1)
$$\begin{cases} \frac{dx(t)}{dt} = s - dx(t) - (1 - \epsilon)\beta x(t)y(t), \\ \frac{dL(t)}{dt} = \alpha_L(1 - \epsilon)\beta x(t)y(t) + (\rho - a - d_L)L(t), \\ \frac{dy(t)}{dt} = (1 - \alpha_L)(1 - \epsilon)\beta x(t)y(t) + aL(t) - \delta y(t) - py(t)z(t), \\ \frac{dz(t)}{dt} = \frac{cy(t)z(t)}{1 + \eta y(t)}K(y) - bz(t), \end{cases}$$

where x denotes activated CD4⁺ T cells, L latently infected cells, y productively infected cells, and z immune cells. Because HIV turnover is more rapid than that of infected cells, we make the quasi-steady assumption by assuming that the viral load is in proportion to the number of infected cells. The parameter s is the generation rate of target cells, and d is the death rate. β is the infection rate and α_L is the fraction of infection that leads to latency. Parameters ρ , a, and d_L are the proliferation rate, activation rate, and death rate of latently infected cells, respectively. The parameter δ is the death rate of productively infected cells and p is the killing rate of infected cells by the immune cells. The overall treatment effectiveness is denoted by ϵ , where $0 \le \epsilon \le 1$. When $\epsilon = 1$, the therapy is 100% effective. If there is no treatment, $\epsilon = 0$ [7, 34]. A saturation term $\frac{cy(t)z(t)}{1+\eta y(t)}$ is used to describe the generation of immune cells due to the infection and b is the death rate of immune cells.

HIV infection can lead to a high level of ROS, causing impairment to the immune response. Inspired by the work by [10, 42, 45, 46], we use $K(y) = \frac{h}{\rho(y)}$ to model the influence of oxidative stress, where $\rho(y) = k + ry$ represents the level of oxidative stress due to the infection. The constant h represents the influence of antioxidant on the immune response, k is the influence of naturally produced oxidant, and r is the influence of oxidant due to infection. It is noted that this immune term incorporates the effect of ROS, which is different from the immune

response and immune impairment term $\frac{cyz}{1+\eta y} - bz - myz$ used in [22, 3, 39, 30], where m is the rate of immune impairment.

The rest of this article is organized as follows. In section 2, we present some preliminary results on the structure of the equilibria of the model. In section 3, we perform stability analysis on the equilibria. In section 4, we analyze bifurcations of the system. In section 5, we study the robustness of the bistable system. We then present sensitive analysis and numerical simulations in section 6. Finally, we conclude the paper in section 7.

2. Preliminary results.

2.1. Positiveness and boundedness. We have the following result on the well-posedness of system (1.1). The proof is given in Appendix A.

Theorem 2.1. System (1.1) has a unique and nonnegative solution with the initial condition $(x^0, L^0, y^0, z^0) \in \mathbb{R}^4_+$, where $\mathbb{R}^4_+ = \{(x_1, x_2, x_3, x_4) | x_j \geq 0, j = 1, 2, 3, 4\}$. Furthermore, the solution is bounded.

2.2. Equilibria and thresholds. In this section, we study the equilibria for system (1.1) and present some threshold values, which will be used to investigate the viral dynamics of model (1.1).

System (1.1) always admits an infection-free equilibrium $E_0 = (x_0, 0, 0, 0)$, where $x_0 = s/d$. Let

$$R_0 = (1 - \epsilon)\beta \left[(1 - \alpha_L) + \frac{a\alpha_L}{a + d_L - \rho} \right] \cdot \frac{s}{d} \cdot \frac{1}{\delta}$$
$$= \frac{s\beta (1 - \epsilon) \left[a\alpha_L + (1 - \alpha_L)(a + d_L - \rho) \right]}{d\delta (a + d_L - \rho)}.$$

Since $(1 - \epsilon)\beta \cdot \frac{s}{d} \cdot \frac{1}{\delta}$ is the basic reproduction number of the model without latent infection, R_0 represents the basic reproduction number of model (1.1). It describes the average number of newly infected cells generated from an infected cell assuming all cells are susceptible.

(i) If $R_0 > 1$, system (1.1) also has an immune-free equilibrium $E_1 = (x_1, L_1, y_1, 0)$, where

$$x_1 = \frac{\delta(a + d_L - \rho)}{\beta(1 - \epsilon) \left[a\alpha_L + (1 - \alpha_L)(a + d_L - \rho) \right]},$$

$$L_1 = \frac{\alpha_L \beta(1 - \epsilon) x_1 y_1}{a + d_L - \rho},$$

$$y_1 = \frac{d(R_0 - 1)}{\beta(1 - \epsilon)}.$$

(ii) We define $h_1 = \frac{br + b\eta k}{c} - \frac{2b\sqrt{\eta rk}}{c}$ and $h_2 = \frac{br + b\eta k}{c} + \frac{2b\sqrt{\eta rk}}{c}$. If $0 < h < h_1$ or $h > h_2$, then $\frac{cyz}{1+\eta y}\frac{h}{k+ry} - bz = 0$ has two positive roots.

Because of the interest in achieving post-treatment control, we only consider $h > h_2$ and call h_2 the post-treatment immune control threshold. In this case, system (1.1) may have two immune equilibria $E_-^* = (x_-^*, L_-^*, y_-^*, z_-^*)$ and $E_+^* = (x_+^*, L_+^*, y_+^*, z_+^*)$, where

$$\begin{split} x_{\pm}^* &= \frac{s}{d + \beta(1 - \epsilon)y_{\pm}^*}, \\ L_{\pm}^* &= \frac{\alpha_L(1 - \epsilon)\beta x_{\pm}^* y_{\pm}^*}{a + d_L - \rho}, \\ y_{\pm}^* &= \frac{B \pm \sqrt{B^2 - 4b^2 kr \eta}}{2b\eta r}, \\ z_{\pm}^* &= \frac{\delta(R_{\pm}^* - 1)}{p}. \end{split}$$

In the positive equilibria, we have

$$\begin{split} R_{\pm}^* &= \frac{s\beta(1-\epsilon)\Big[(1-\alpha_L) + \frac{a\alpha_L}{a+d_L-\rho}\Big]}{\delta\Big[d + \frac{b\beta(1-\epsilon)}{\frac{B\pm\sqrt{B^2-4b^2kr\eta}}{2k}}\Big]} \\ &= \frac{2b\eta rs\beta(1-\epsilon)\Big[a\alpha_L + (a+d_L-\rho)(1-\alpha_L)\Big]}{\delta(a+d_L-\rho)\Big\{2b\eta rd + \beta(1-\epsilon)\Big[B\pm\sqrt{B^2-4b^2kr\eta}\Big]\Big\}}, \end{split}$$

where $B = ch - br - bk\eta$. It can be calculated that $\frac{s\beta(1-\epsilon)}{\delta[d+\frac{b\beta(1-\epsilon)}{2}]}$ is the basic immune reproduction number of the model with the bilinear immune incidence (cyz) and without the latent reservoir. Here, R_{\pm}^* represent the two additional threshold parameters, which can characterize the dynamics of the model, that is, E_{\pm}^* exists when $R_{\pm}^* > 1$.

Let
$$R_c = 1 + \frac{\beta(1-\epsilon)\sqrt{\eta rk}}{dr\eta}$$
. We define

$$h^* = \frac{br + b\eta k}{c} + \frac{2b\eta r y_1}{c}$$

and the elite control threshold

$$h^{**} = \frac{br + b\eta k}{c} + \frac{bk\beta(1 - \epsilon)}{cd(R_0 - 1)} + \frac{bd\eta r(R_0 - 1)}{c\beta(1 - \epsilon)}.$$

Then we have the following results with straightforward calculation.

Lemma 2.2. We state that
$$R_0 > R_c \Leftrightarrow h^* > h^{**} \Leftrightarrow h^* > h_2 \Leftrightarrow y_1 > \sqrt{\frac{k}{\eta r}}$$
.

Lemma 2.3.

- $\begin{array}{l} \text{(i)} \ \textit{If} \ R_c > R_0 > 1, \ then \ R_+^* > 1 \ \textit{has no solution, and} \ R_-^* > 1 \Leftrightarrow h > h^{**}. \\ \text{(ii)} \ \textit{If} \ R_0 > R_c > 1, \ then \ R_+^* > 1 \Leftrightarrow h_2 < h < h^{**}, \ \textit{and} \ R_-^* > 1 \Leftrightarrow h > h_2. \end{array}$

Based on Lemmas 2.2 and 2.3, combining the aforementioned analysis leads to the existence results regarding the equilibria of system (1.1). The results for positive equilibria are summarized in Tables 1 and 2.

Theorem 2.4.

- (i) System (1.1) always admits an uninfected equilibrium E_0 .
- (ii) If $R_0 > 1$, system (1.1) also has an immune-free equilibrium E_1 .

Table 1
The existence of the positive equilibria when $R_c > R_0 > 1$.

	$h_2 < h < h^{**}$	$h > h^{**}$
E_{-}^{*}	_	Exist
E_+^*	_	_

Table 2
The existence of the positive equilibria when $R_0 > R_c > 1$.

	$h_2 < h < h^{**}$	$h > h^{**}$
E_{-}^{*}	Exist	Exist
E_+^*	Exist	

- (iii) Suppose that $R_c > R_0 > 1$. When $h > h^{**}$, system (1.1) has only one positive equilibrium E_-^* .
- (iv) Suppose that $R_0 > R_c > 1$. When $h_2 < h < h^{**}$, system (1.1) has two positive equilibria E_-^* and E_+^* ; when $h > h^{**}$, system (1.1) has only one positive equilibrium E_-^* ; when $h = h_2$, system (1.1) has a coinciding equilibrium E_* .
- **3. Stability analysis.** In this section, we consider the stability of equilibria for system (1.1).

Let \tilde{E} be any arbitrary equilibrium of system (1.1) and denote

$$\mathscr{J} = \begin{bmatrix} -d - \beta(1-\epsilon)\tilde{y} & 0 & -\beta(1-\epsilon)\tilde{x} & 0\\ \alpha_L\beta(1-\epsilon)\tilde{y} & \rho - a - d_L & \alpha_L(1-\epsilon)\beta\tilde{x} & 0\\ (1-\alpha_L)\beta(1-\epsilon)\tilde{y} & a & (1-\alpha_L)\beta(1-\epsilon)\tilde{x} - \delta - p\tilde{z} & -p\tilde{y}\\ 0 & 0 & \frac{ch\tilde{z}(k-\eta r\tilde{y}^2)}{(1+\eta\tilde{y})^2(k+r\tilde{y})^2} & \frac{ch\tilde{y}}{(1+\eta\tilde{y})(k+r\tilde{y})} - b \end{bmatrix}.$$

The characteristic equation of the linearized system of (1.1) at \tilde{E} is then obtained as

$$(3.1) Det(\lambda I - \mathcal{J}) = 0,$$

where Det means the determinant of a matrix and λ is the eigenvalue.

3.1. Stability analysis of equilibrium E_0 .

Theorem 3.1. If $R_0 < 1$, then the uninfected equilibrium E_0 of system (1.1) is locally asymptotically stable. If $R_0 > 1$, E_0 is unstable.

Theorem 3.2. If $R_0 < 1$, then the uninfected equilibrium E_0 of system (1.1) is global asymptotically stable.

The proofs of these theorems are given in Appendices B and C. The global asymptotic stability of the uninfected equilibrium E_0 in system (1.1) shows that the virus will eventually be cleared within the host. In general, when treatment is sufficiently effective, we have $R_0 < 1$, indicating the eradication of the virus.

Table 3
The stability of the equilibria and the behavior of system (1.1) under assumption $A_3(A_1A_2 - A_3) - A_1^2A_4 > 0$.

	E_0	E_1	E_{-}^{*}	E_+^*	System (1.1)
$R_0 < 1$	GAS	_	_	_	Tends to E_0
$R_c > R_0 > 1.0 < h < h^{**}$	US	LAS	_		Tends to E_1
$R_c > R_0 > 1, h > h^{**}$	US	US	LAS	_	Tends to E_{-}^{*}

Table 4
The stability of the equilibria and the behavior of system (1.1) under assumption $A_3(A_1A_2 - A_3) - A_1^2A_4 > 0$.

	E_0	E_1	E_{-}^{*}	E_+^*	System (1.1)
$R_0 < 1$	GAS		_		Tends to E_0
$R_0 > 1, \ 0 < h < h_2,$	US	LAS		_	Tends to E_1
$R_0 > R_c > 1, h_2 < h < h^{**}$	US	LAS	LAS	US	Bistable
$R_0 > R_c > 1, h > h^{**}$	$_{ m US}$	US	LAS	_	Tends to E_{-}^{*}

3.2. Stability of equilibrium E_1 .

Theorem 3.3. Assume $R_0 > 1$. If $0 < h < h^{**}$, then the immune free equilibrium E_1 of system (1.1) is locally asymptotically stable. If $h > h^{**}$, E_1 is unstable.

The proof is given in Appendix D. From this analysis, we know that the elite control threshold h^{**} plays a crucial role in determining whether a system is under elite control, as described by [7].

3.3. Stability of positive equilibria.

Theorem 3.4. (i) Suppose that (**A**) $A_3(A_1A_2 - A_3) - A_1^2A_4 > 0$. If we further assume (**A.1**) $1 < R_0 < R_c$ and $h > h^{**}$ or (**A.2**) $R_0 > R_c$ and $h > h_2$, then system (1.1) has a positive equilibrium E_-^* , which is a stable node.

(ii) If $R_0 > R_c$ and $h_2 < h < h^{**}$, system (1.1) also has a positive equilibrium E_+^* , which is an unstable saddle point.

The proof is given in Appendix E. The stability of the equilibria and the behavior of system (1.1) are summarized in Tables 3 and 4. In those tables, US, LAS, and GAS represent unstable, locally asymptotically stable and global asymptotically stable, respectively.

4. Bifurcations analysis.

4.1. Saddle-node bifurcation. In section 2.3, we have discussed the conditions for the existence of equilibria, namely E_-^* and E_+^* . If $R_0 > R_c > 1$ and $h > h_2$, system (1.1) possesses two positive equilibria. On the other hand, if h is smaller than h_2 , the system will not have any positive equilibria. When h is equal to h_2 , the system will exhibit a unique positive equilibrium denoted as $E_* = (x_*, L_*, y_*, z_*)$, where $y_* = \sqrt{\frac{k}{\eta r}}$. The disappearance or emergence of the positive equilibria is attributed to a saddle-node bifurcation, which occurs at $h^{[sn]}$, defined as $h^{[sn]} = h_2 = \frac{br + b\eta k}{c} + \frac{2b\sqrt{\eta rk}}{c}$. We prove it in the following theorem.

Theorem 4.1. If $R_0 > R_c > 1$ and $h = h^{[sn]}$, system (1.1) undergoes a saddle-node bifurcation around E_* .

Proof. We utilize Sotomayor's theorem to establish the occurrence of a saddle-node bifurcation in system (1.1) near $h^{[sn]}$. Proving $Det[\mathscr{J}_{E_*}] = 0$ is not challenging, which implies the presence of a zero eigenvalue in the Jacobian matrix evaluated at E_* .

Let $V = (V_1, V_2, V_3, V_4)^T$ and $W = (W_1, W_2, W_3, W_4)^T$ represent the eigenvectors of \mathscr{J}_{E_*} and $\mathscr{J}_{E_*}^T$ corresponding to the zero eigenvalue, respectively. Then we have

$$\begin{split} W &= \begin{bmatrix} W_1 \\ W_2 \\ W_3 \\ W_4 \end{bmatrix} = \begin{bmatrix} 0 \\ 0 \\ 0 \\ 1 \end{bmatrix}, \\ V &= \begin{bmatrix} V_1 \\ V_2 \\ V_3 \\ V_4 \end{bmatrix} = \begin{bmatrix} 1 \\ \frac{\alpha_L d}{\rho - a - d_L} \\ -\frac{d + \beta(1 - \epsilon)y_*}{\beta(1 - \epsilon)x_*} \\ \frac{[(\delta + pz_*)[d + \beta(1 - \epsilon)y_*] - \beta dx_*(1 - \alpha_L)(1 - \epsilon)](\rho - a - d_L) + \alpha_L \beta ad(1 - \epsilon)x_*}{\beta py_*(\rho - a - d_L)(1 - \epsilon)x_*} \end{bmatrix} \end{split}$$

Let $F = (f_1, f_2, f_3, f_4)$ represent the right-hand side of system (1.1). Then we get

$$F_h(E_*; h^{[sn]}) = \begin{bmatrix} 0 \\ 0 \\ 0 \\ \frac{cy_*z_*}{(1+\eta y_*)(k+ry_*)} \end{bmatrix}$$

and

$$D^{2}F(E_{*};h^{[sn]})(V,V) = \begin{bmatrix} -2(1-\epsilon)\beta V_{1}V_{3} \\ 2\alpha_{L}(1-\epsilon)\beta V_{1}V_{3} \\ -2pV_{3}V_{4} + 2(1-\alpha_{L})(1-\epsilon)\beta V_{1}V_{3} \\ \frac{-2cz_{*}h(3\eta rky_{*} + k^{2}\eta + rk - \eta^{2}r^{2}(y_{*})^{3})}{(1+\eta y_{*})^{3}(k+ry_{*})^{3}}V_{3}^{2} \end{bmatrix}.$$

Therefore, we obtain

$$\begin{split} &\Omega_1 = W^{\mathrm{T}} F_h(E_*; h^{[sn]}) = \frac{cy_* z_*}{(1 + \eta y_*)(k + ry_*)} \neq 0, \\ &\Omega_2 = W^{\mathrm{T}} [D^2 F(E_*; h^{[sn]})(V, V)] = \frac{-2ch z_* (3\eta r k y_* + k^2 \eta + rk - \eta^2 r^2 y_*^3)}{(1 + \eta y_*)^3 (k + ry_*)^3} V_3^2 \neq 0. \end{split}$$

Therefore, system (1.1) undergoes a saddle-node bifurcation at E_* when $h = h^{[sn]}$. When $h < h^{[sn]}$, there is no positive equilibrium. When $h > h^{[sn]}$, there are two positive equilibria.

4.2. Backward and forward bifurcations. The above analysis implies that when $R_0 > R_c > 1$ and $h = \frac{br + b\eta k}{c} + \frac{bk\beta(1-\epsilon)}{cd(R_0-1)} + \frac{bd\eta r(R_0-1)}{c\beta(1-\epsilon)}$, the immune-free equilibrium E_1 will lose its stability, and the characteristic equation at E_1 has a zero eigenvalue. Therefore, bifurcation may occur at E_1 . Next, we will take h as the bifurcation parameter and study backward and forward bifurcations.

Theorem 4.2. If $R_0 > R_c > 1$ and $h = h^{**}$, system (1.1) undergoes a backward bifurcation. The bifurcation parameter is $h = h^{**} = \frac{br + b\eta k}{c} + \frac{bk\beta(1-\epsilon)}{cd(R_0-1)} + \frac{bd\eta r(R_0-1)}{c\beta(1-\epsilon)}$.

Proof. We use the Castillo-Chavez and Song theorem [6] to prove the existence of the backward bifurcation at $h = h^{[tb]}$. It is easy to prove that $Det[\mathscr{J}_{E_1}] = 0$ at $h = h^{[tb]}$, which implies that one of the eigenvalues of the Jacobian at E_1 is zero. Let $v = (v_1, v_2, v_3, v_4)^T$ and $w = (w_1, w_2, w_3, w_4)$ represent the right and left eigenvector of \mathscr{J}_{E_1} corresponding to the zero eigenvalue, respectively. Then we have

$$v = \begin{bmatrix} v_1 \\ v_2 \\ v_3 \\ v_4 \end{bmatrix} = \begin{bmatrix} 1 \\ \frac{\alpha_L d}{\rho - a - d_L} \\ -\frac{d + \beta(1 - \epsilon)y_1}{\beta(1 - \epsilon)x_1} \\ -\frac{\delta d}{ps} \end{bmatrix}.$$

The left eigenvector w satisfying $v \cdot w = 1$ is

$$w^T = \begin{bmatrix} w_1 \\ w_2 \\ w_3 \\ w_4 \end{bmatrix} = \begin{bmatrix} 0 \\ 0 \\ 0 \\ -\frac{ps}{\delta d} \end{bmatrix}.$$

Then we get

$$D^{2}F(E_{1}; h^{[tb]})(v, v)$$

$$= \begin{bmatrix}
-2(1 - \epsilon)\beta v_{1}v_{3} \\
2\alpha_{L}(1 - \epsilon)\beta v_{1}v_{3} \\
-2pv_{3}v_{4} + 2(1 - \alpha_{L})(1 - \epsilon)\beta v_{1}v_{3} \\
\frac{2ch(k - \eta ry_{1}^{2})}{(1 + \eta y_{1})^{2}(k + ry_{1})^{2}}v_{3}v_{4}
\end{bmatrix}$$

and

Therefore, we have

$$a = w \cdot [D^2 F(E_1; h^{[tb]})(v, v)] = \frac{2ch(k - \eta r y_1^2)}{(1 + \eta y_1)^2 (k + r y_1)^2} w_4 v_3 v_4,$$

$$b = w \cdot T[DF_h(E_1; h^{[tb]})v] = \frac{cy_1}{(1 + \eta y_1)(k + r y_1)} w_4 v_4.$$

It is clear that $w_4v_4=1>0$ and b>0. It follows from Lemma 2.2 that $y_1>\sqrt{\frac{k}{\eta r}}$ when $R_0>R_c$. Thus, $k-\eta ry_1^2<0$ and $w_4v_3v_4=-\frac{d+\beta(1-\epsilon)y_1}{\beta(1-\epsilon)x_1}<0$. We then get a>0. From Corollary 4.1 in [6], we know that both a and b are positive. Therefore, system (1.1) undergoes a backward bifurcation at $h=h^{**}$.

When $1 < R_0 < R_c$, the direction of the bifurcation in system (1.1) will change from backward to forward.

Theorem 4.3. If $1 < R_0 < R_c$ and $h = h^{**}$, system (1.1) undergoes a forward bifurcation. The bifurcation parameter is $h = h^{**} = \frac{br + b\eta k}{c} + \frac{bk\beta(1-\epsilon)}{cd(R_0-1)} + \frac{bd\eta r(R_0-1)}{c\beta(1-\epsilon)}$.

Proof. From Lemma 2.2, we know that $y_1 < \sqrt{\frac{k}{\eta r}}$ when $1 < R_0 < R_c$, which implies that $k - \eta r y_1^2 > 0$. Thus, from the proof of Theorem 4.2, when $1 < R_0 < R_c$, we get

$$a = w \cdot [D^2 F(E_1; h^{[tb]})(v, v)] = \frac{2ch(k - \eta r y_1^2)}{(1 + \eta y_1)^2 (k + r y_1)^2} w_4 v_3 v_4 < 0$$

and

$$b = w \cdot T[DF_h(E_1; h^{[tb]})v] = \frac{cy_1}{(1 + \eta y_1)(k + ry_1)} w_4 v_4 > 0.$$

Therefore, from Theorem 4.1 in [6], when a < 0 and b > 0, system (1.1) undergoes a forward bifurcation at $h = h^{**}$.

5. Robustness of bistability. The system exhibiting a backward bifurcation is bistable, meaning it possesses two basins of attraction [9, 38]. Here we define the robustness of the bistable system (1.1) as the area under the positive steady solution curve within the interval $[h_2, h^{**}]$, representing one basin of attraction. The robustness associated with variable y in the bistable system (1.1) can be computed by

$$R_{y} = \int_{h_{2}}^{h^{**}} y_{+}^{*} dh$$

$$= \int_{h_{2}}^{h^{**}} \left(\frac{B + \sqrt{B^{2} - 4b^{2}kr\eta}}{2b\eta r} \right) dh$$

$$= \int_{h_{2}}^{h^{**}} \left(\frac{ch - br - bk\eta + \sqrt{(ch - br - bk\eta)^{2} - 4b^{2}kr\eta}}{2b\eta r} \right) dh,$$

and the robustness associated with L is

$$R_{L} = \int_{h_{2}}^{h^{**}} L_{+}^{*} dh$$

$$= \int_{h_{2}}^{h^{**}} \left(\frac{\alpha_{L} (1 - \epsilon) \beta x_{+}^{*} y_{+}^{*}}{a + d_{L} - \rho} \right) dh.$$

For instance, the cyan-colored area depicted in Figures 3, 7, and 8 represents R_y , which corresponds to the robustness of variable y in the bistable system (1.1). Similarly, the cyan-colored area shown in Figures 4, 9, and 10 represents R_L , the robustness corresponding to variable L in the bistable system (1.1).

Table 5

The robustness R_y and R_L for the bistable system (1.1) with different values of k (the influence of naturally produced oxidant). Other parameter values are listed in Table 7.

\overline{k}	R_y	R_L
0.8	1.1418	2.6680
0.9	1.0589	2.4535
1.0	0.9816	2.2565
1.1	0.9093	2.0750
1.2	0.8415	1.9072

Table 6

The robustness R and R_L for the bistable system (1.1) with different values of r (the influence of oxidant produced by infected $CD4^+$ T cells or HIV viral load). Other parameter values are listed in Table 7.

\underline{r}	R_y	R_L
0.1	0.9816	2.2565
0.2	2.8639	6.8995
0.3	4.8900	12.0462
0.4	6.9751	17.4191
0.5	9.0924	22.9228

The robustness measures R_y and R_L reflect the resistance to virus rebound. A larger value of R_y or R_L indicates a stronger robustness in the bistable system. A stronger robustness means that it is more challenging for the virus to rebound.

To investigate the influence of parameters k and r on the robustness of the bistable system (1.1), we calculate the robustness values R_y and R_L for different parameter values of k and r. The corresponding results are presented in Figures 7 to 10 and Tables 5 and 6. We observe that as the value of k (representing the impact of naturally produced oxidant) increases, the robustness of the bistable system (1.1) decreases, indicating a higher likelihood of virus rebound. Conversely, a larger value of r (representing the influence of oxidant produced by infected CD4⁺ T cells or HIV viral load) leads to better robustness in the bistable system (1.1), indicating a lower likelihood of virus rebound.

6. Sensitivity analysis and numerical simulations.

6.1. Sensitivity analysis. Sensitivity analysis is a widely employed technique to examine the impact of various parameters on the basic reproductive number, R_0 , in epidemic models [41]. In this study, we conduct sensitivity analysis to investigate the relationship between R_0 and the basic immune reproductive number, R_-^* , as well as the system parameters in our model. Latin hypercube sampling (LHS) and partial rank correlation coefficients (PRCCs) are utilized for this purpose [2, 23]. LHS is a statistical sampling method that efficiently explores parameter variations within specified uncertainty ranges for each parameter [2]. On the other hand, PRCCs indicate the level of significance associated with each parameter. PRCCs are calculated using rank-transformed LHS matrices and output matrices [23]. For our analysis, we conducted 4000 simulations per run and employed a uniform distribution function to evaluate the significance of PRCCs for all parameters, considering their wide ranges.

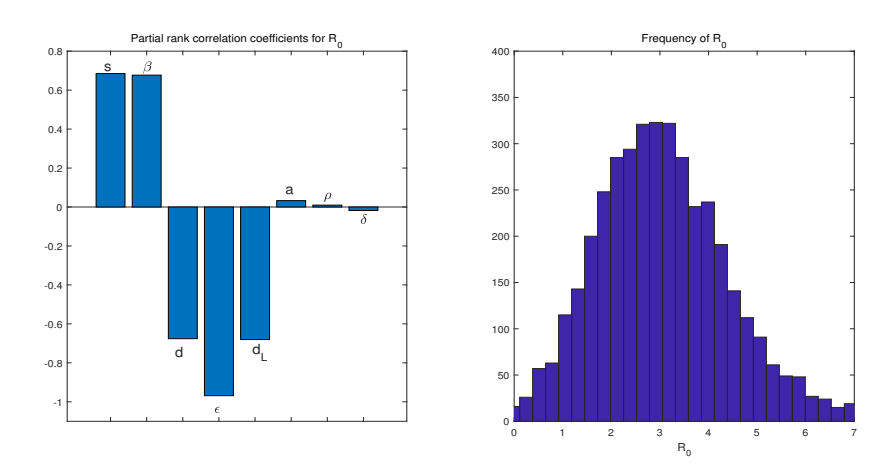


Figure 1. Partial rank correlation coefficients illustrate the dependence of R_0 for system (1.1) on each parameter, along with the frequency distribution of R_0 .

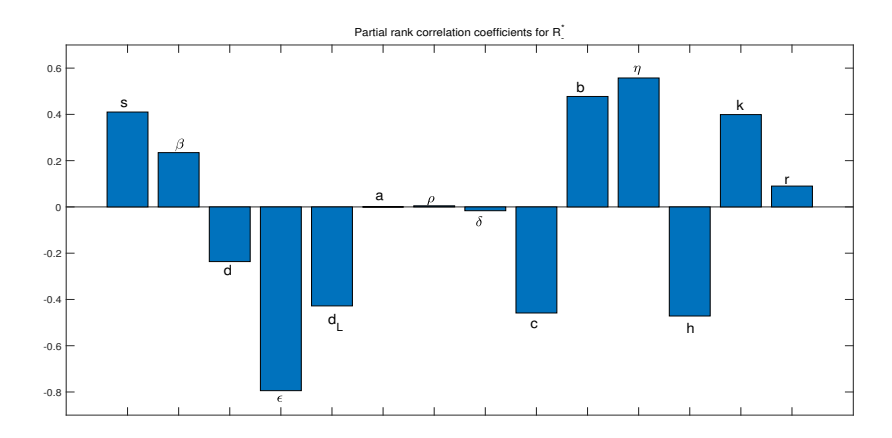


Figure 2. Partial rank correlation coefficients illustrate the dependence of R_{-}^{*} for system (1.1) on each parameter.

The PRCC results presented in Figures 1 and 2 depict the relationship between R_0 and R_-^* with each system parameter, and provide an estimation of the normal distributions for these variables. When the absolute value of PRCC exceeds 0.4, it indicates a significant correlation between the input parameters and the output variables. Correlations ranging between 0.2 and 0.4 represent moderate correlations. For PRCC values within the range of [0, 0.2], the correlations are weak.

Upon analysis, we observe that the proliferation rate of CD4⁺ T cells (s), the decay rate of CD4⁺ T cells (d), the infection rate of CD4⁺ T cells (β), the drug efficacy (ϵ), and the latently infected cell death rate (d_L) significantly influence the infection reproduction number (R_0) and the immune reproduction number (R_-^*).

6.2. Numerical simulations. In this section, we conducted some numerical simulations using the default parameter values listed in Table 7. We acknowledged that certain parameter values, specifically those associated with oxidative stress, were chosen for the purpose of illustrating the dynamics as no prior data were available.

Table 7Parameters for system (1.1).

Symbol description	Value	Reference
s Proliferation rate of CD4 ⁺ T cells	$10 \text{ cells}/\mu \text{ L/ day}$	[4]
d Decay rate of CD4 ⁺ T cells	$0.01 \mathrm{day}^{-1}$	[4]
β Infection rate of CD4 ⁺ T cells	$0.015~\mu$ L/ day	_
ϵ Drug efficacy	0.8	_
α_L Fraction of newly infected cells that become latently infected	0.001	_
ρ Proliferation rate of latently infected cells	0.0045 day^{-1}	[7]
a Activation rate	0.001 day^{-1}	[7]
d_L Death rate of latently infected cells	$0.004 \mathrm{day^{-1}}$	[7]
δ Death rate of infected cells	$1 \mathrm{day}^{-1}$	[7]
p Killing rate of infected CD4 ⁺ T cells	$0.1 \mathrm{day^{-1}}$	_
c Proliferation rate of CTLs	$0.1 \mathrm{day^{-1}}$	_
η Effector cell production hill function scaling	$1 \text{ cells}/\mu \text{ L}$	_
b Decay rate of CTLs	$0.1 \mathrm{day}^{-1}$	_
h Antioxidant parameter	$1.8 \ day^{-1}$	_
k The natural oxidant content	$1 \text{ cells}/\mu \text{ L}$	_
r Oxidant content induced by HIV	$0.1 \text{ cells}/\mu L$	_

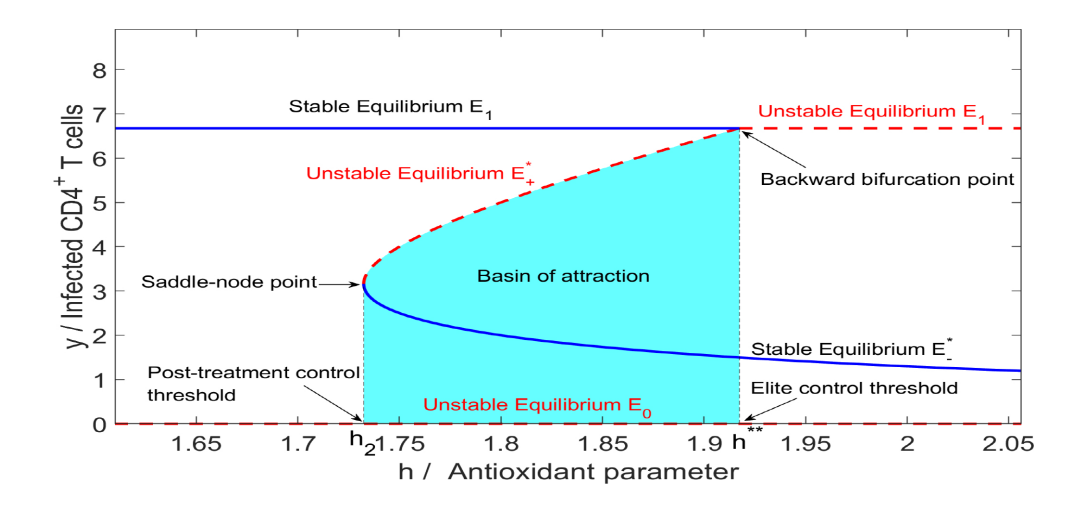


Figure 3. Bistability and bifurcation diagram of system (1.1) where the vertical axis represents y (infected $CD4^+$ T cells). The bistable interval is (1.7325, 1.9174). When h < 1.7325, the model exhibits a steady state with high viral load, indicating viral rebound. Conversely, when h > 1.9174, the model displays a steady state with low viral load, indicating elite control in patients. When h is between these two values, the model exhibits bistability depending on the initial conditions, such as the size of infected cells or immune cells at the time of treatment cessation. By choosing h as the bifurcation parameter, system (1.1) undergoes a saddle-node bifurcation at $h = h_2$ and a backward bifurcation at $h = h^{**}$. The parameter values can be found in Table 7. The cyan area represents the robustness $R_y = 0.9816$ for the bistable system. (Figure in color online.)

With these default parameters, we obtained the following threshold values: $R_0 \approx 3.0030$, $R_c \approx 2.0392 < R_0$, $h_2 \approx 1.7325$, and $h^{**} \approx 1.9174$. The bistable interval was found to be (1.7325, 1.9174). From Figures 3 and 4, it can be observed that there is no positive equilibrium for h < 1.7325, and a saddle-node bifurcation occurs when h passes through 1.7325. Additionally, system (1.1) exhibits a backward bifurcation when h passes through 1.9174.

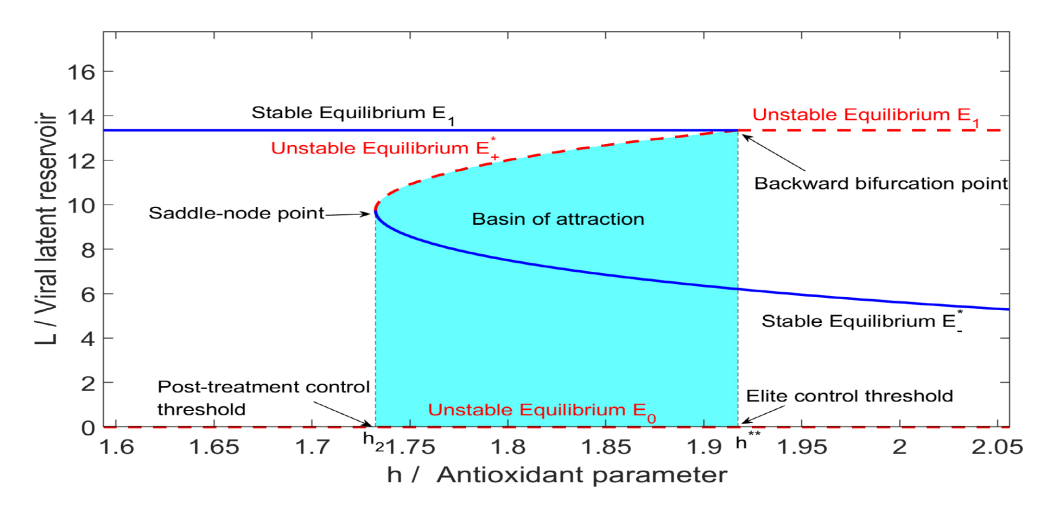


Figure 4. Bistability and bifurcation diagram of system (1.1) where the vertical axis represents L (viral latent reservoir). The bistable interval is (1.7325, 1.9174). When h < 1.7325, the model exhibits a steady state with a high viral latent reservoir, indicating viral rebound. Conversely, when h > 1.9174, the model displays a steady state with a low viral latent reservoir, indicating elite control in patients. When h is between these two values, the model exhibits bistability depending on the initial conditions, such as the size of infected cells or immune cells at the time of treatment cessation. By choosing h as the bifurcation parameter, system (1.1) undergoes a saddle-node bifurcation at $h = h_2$ and a backward bifurcation at $h = h^{**}$. The parameter values can be found in Table 7. The cyan area represents the robustness $R_L = 2.2565$ for the bistable system. (Figure in color online.)

If we set $\delta=2$ while keeping the other parameter values listed in Table 7, we obtain $R_0\approx 1.5015,\ R_c\approx 2.0392>R_0,\ h_2\approx 3.4798,$ and $h^{**}\approx 3.5522.$ As shown in Figures 5 and 6, there is no positive equilibrium for h<3.5522, and a forward bifurcation occurs when h passes through 3.5522. Figure 11 illustrates that when $h_2< h< h^{**},$ system (1.1) has two stable equilibria.

Furthermore, we investigated the influence of system parameters on the virus rebound threshold h_2 and the elite control threshold h^{**} . From the PRCCs in Figure 12, we can observe that the decay rate of CTLs (b), the effector cell production hill function scaling (η) , and the natural oxidant content (k) are significantly positively correlated with the virus rebound threshold h_2 . Conversely, the proliferation rate of CTLs (c) is significantly negatively correlated with the virus rebound threshold h_2 .

Figure 13 indicates that the activation rate of infected cell death (δ) is significantly negatively correlated with the elite control threshold h^{**} , while the proliferation rate of latently infected cells (ρ) is significantly positively correlated with the elite control threshold h^{**} . Biologically, an increased decay rate of CTLs, effector cell production hill function scaling, and natural oxidant content make it more challenging to treat the disease. Conversely, an increased proliferation rate of CTLs is beneficial for disease treatment.

The phenomenon of bistability can also arise in other HIV infection models that involve oxidative stress. As an example, we investigated the HIV infection model (6.1) with a logistic proliferation rate of latently infected cells. Through simulations, we demonstrated the existence of bistability. Figure 14 shows that system (6.1) exhibits bistable behavior for different

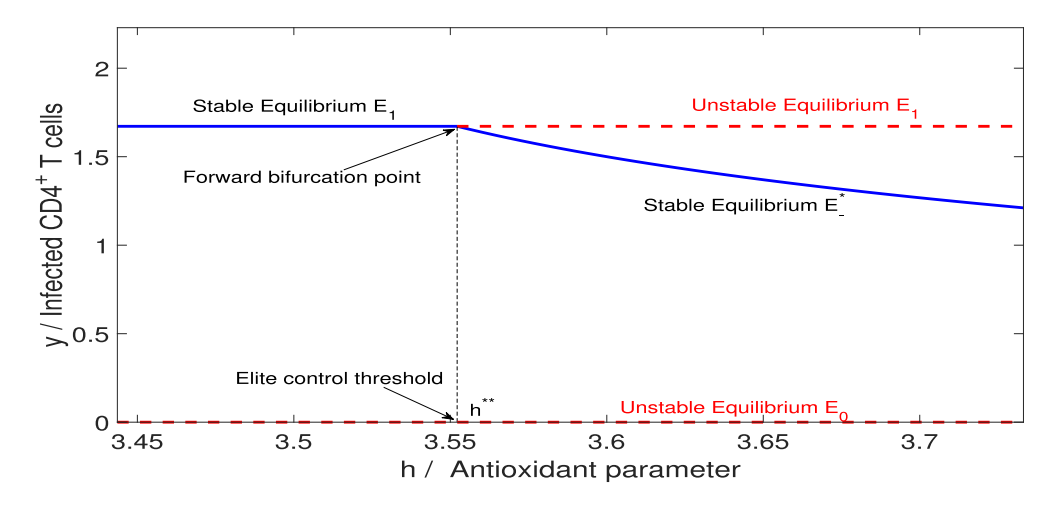


Figure 5. Bifurcation diagram of system (1.1) where the vertical axis represents y (infected CD4⁺ T cells). When h < 3.5522, the model exhibits a steady state with a high viral load, indicating viral rebound. Conversely, when h > 3.5522, the model displays a steady state with a low viral load, indicating elite control in patients. By choosing h as the bifurcation parameter, system (1.1) undergoes a forward bifurcation at $h = h^{**}$. In this diagram, we set $\delta = 2$ day⁻¹ while keeping the other parameter values as shown in Table 7.

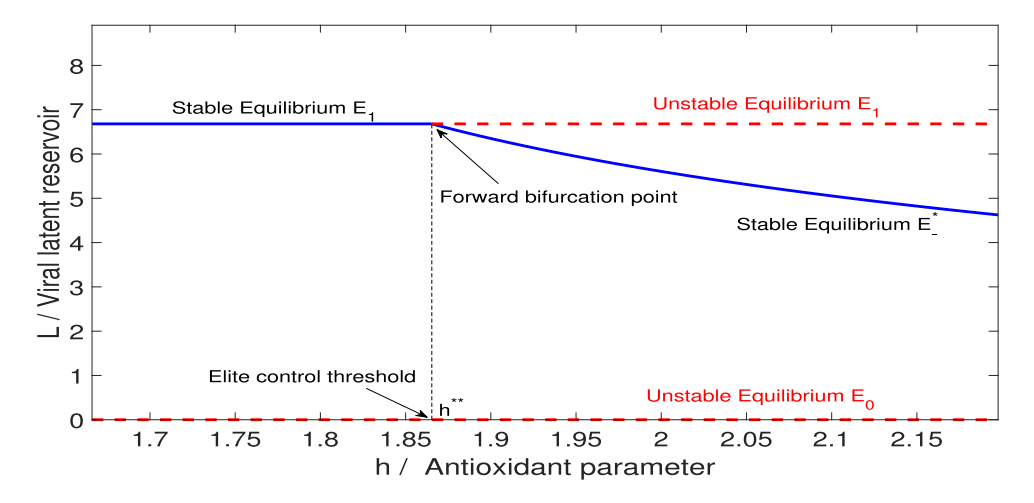


Figure 6. Bifurcation diagram of system (1.1) where the vertical axis represents L (viral latent reservoir). When h < 3.5522, the model exhibits a steady state with a high viral latent reservoir, indicating viral rebound. Conversely, when h > 3.5522, the model displays a steady state with a low viral latent reservoir, indicating elite control in patients. By choosing h as the bifurcation parameter, system (1.1) undergoes a forward bifurcation at $h = h^{**}$. In this diagram, we set $\delta = 2$ day⁻¹ while keeping the other parameter values as shown in Table 7.

initial values when $L_{\text{max}} = 50$ (with the values of other parameters listed in Table 12). We then have

(6.1)
$$\begin{cases} \frac{dx(t)}{dt} = s - dx(t) - (1 - \epsilon)\beta x(t)y(t), \\ \frac{dL(t)}{dt} = \alpha_L(1 - \epsilon)\beta x(t)y(t) - (a + d_L)L(t) + \rho L(t)(1 - \frac{L(t)}{L_{max}}), \\ \frac{dy(t)}{dt} = (1 - \alpha_L)(1 - \epsilon)\beta x(t)y(t) + aL(t) - \delta y(t) - py(t)z(t), \\ \frac{dz(t)}{dt} = \frac{cy(t)z(t)}{1 + \eta y(t)} \frac{h}{k + ry(t)} - bz(t). \end{cases}$$

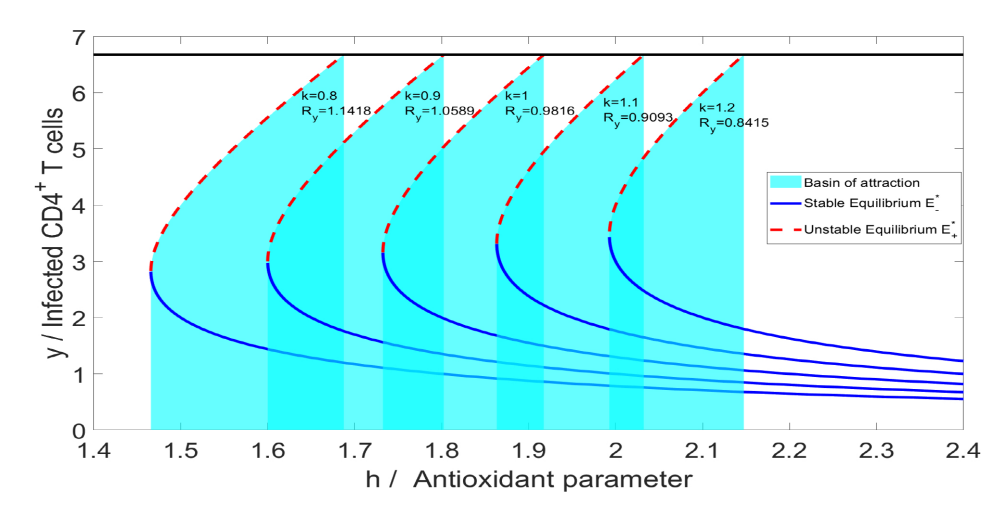


Figure 7. Bistability and bifurcation diagram of system (1.1) with different values of k (the influence of naturally produced oxidant), where the vertical axis represents y (infected CD4⁺ T cells). The parameter values for the other variables are shown in Table 7. The cyan-colored area represents the robustness R_y of the bistable system. (Figure in color online.)

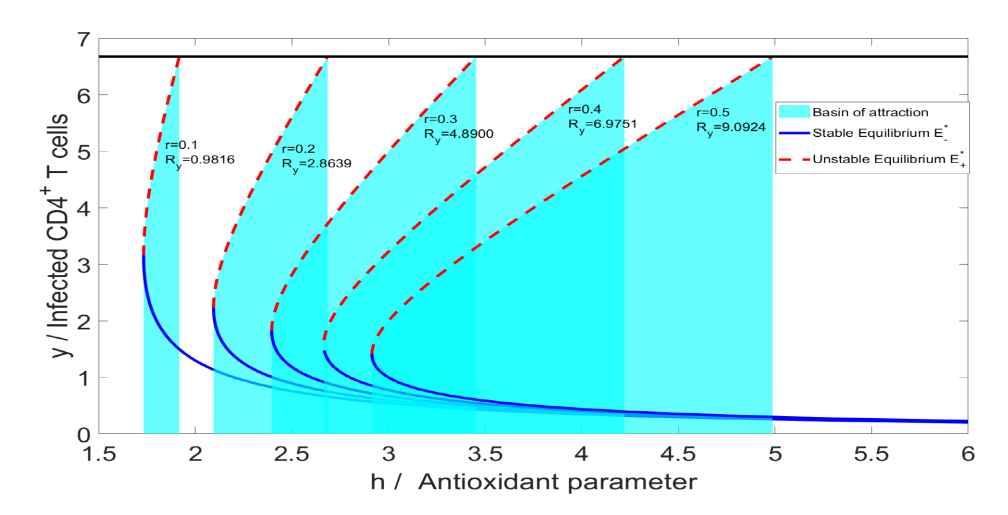


Figure 8. Bistability and bifurcation diagram of system (1.1) with different values of r (the influence of oxidant produced by infected $CD4^+$ T cells or HIV viral load), where the vertical axis represents y (infected $CD4^+$ T cells). The parameter values for the other variables are shown in Table 7. The cyan-colored area denotes the robustness R_y of the bistable system. (Figure in color online.)

7. Conclusion. In this paper, we propose a simplified within-host model to investigate the mechanisms of post-treatment immune control and elite control in HIV infection. We determine the thresholds for post-treatment immune control and elite control within the model and demonstrate that the model exhibits a diverse range of dynamic behaviors. Through sensitivity analysis and numerical simulations, we discover that reducing the immune impairment rate is advantageous for the host to achieve post-treatment immune control and elite control. Specifically, a therapeutic approach aimed at decreasing the immune impairment rate of the

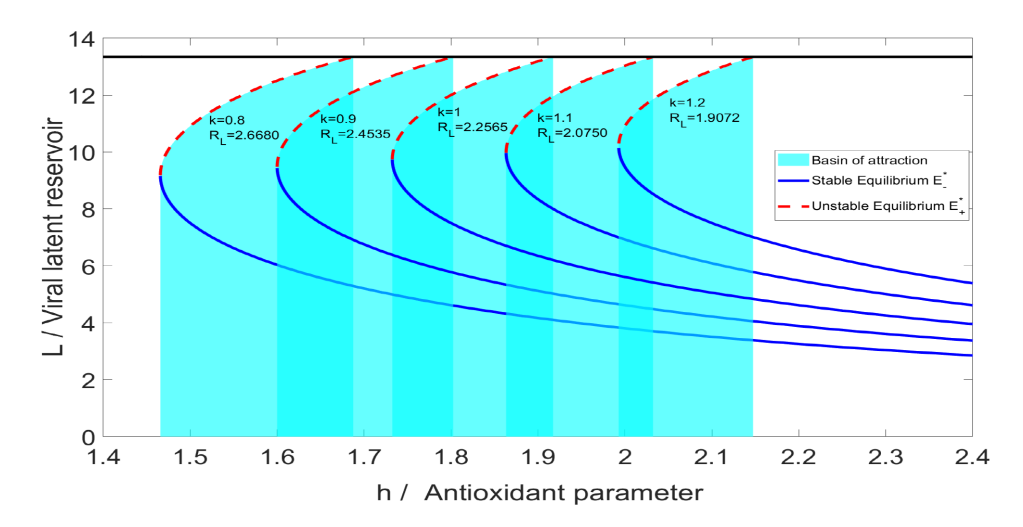


Figure 9. Bistability and bifurcation diagram of system (1.1) with different values of k (the influence of naturally produced oxidant), where the vertical axis represents L (viral latent reservoir). The parameter values for the other variables are shown in Table 7. The cyan-colored area denotes the robustness R_L of the bistable system. (Figure in color online.)

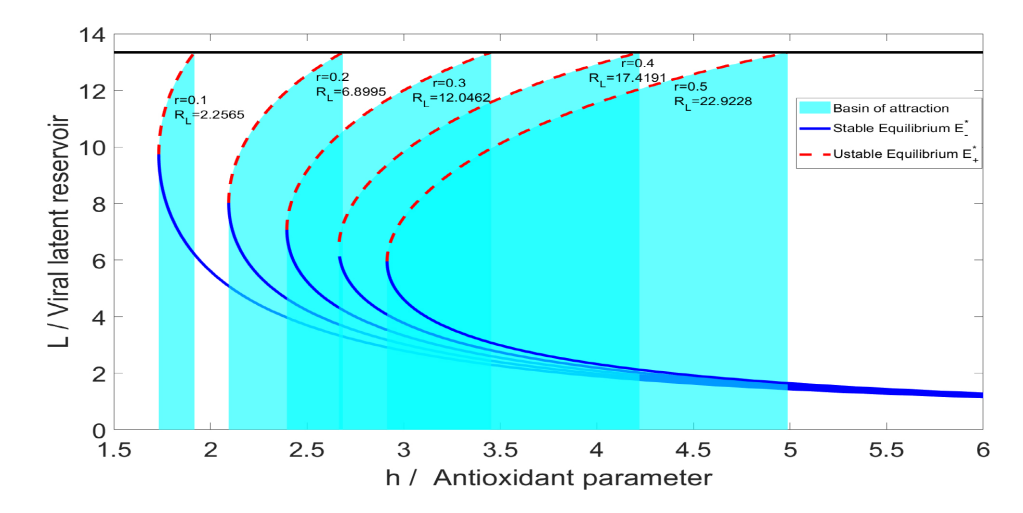


Figure 10. Bistability and bifurcation diagram of system (1.1) with different values of r (the influence of oxidant produced by infected $CD4^+$ T cells or HIV viral load), where the vertical axis represents L (viral latent reservoir). The parameter values for the other variables are shown in Table 7. The cyan-colored area denotes the robustness R_L of the bistable system. (Figure in color online.)

virus, as well as the decay rate of CTLs and the effector cell production hill function scaling, can significantly enhance the host's ability to achieve elite control. These findings hold potential for practical applications in the design of optimal treatment strategies for relevant diseases. We also note that oxidative stress is a common feature observed across various viral infections, including hepatitis B, C, and delta viruses, as well as herpes and respiratory viruses [15]. The modeling process and analysis methods employed in this study may be applied to these viral infections and immune responses.

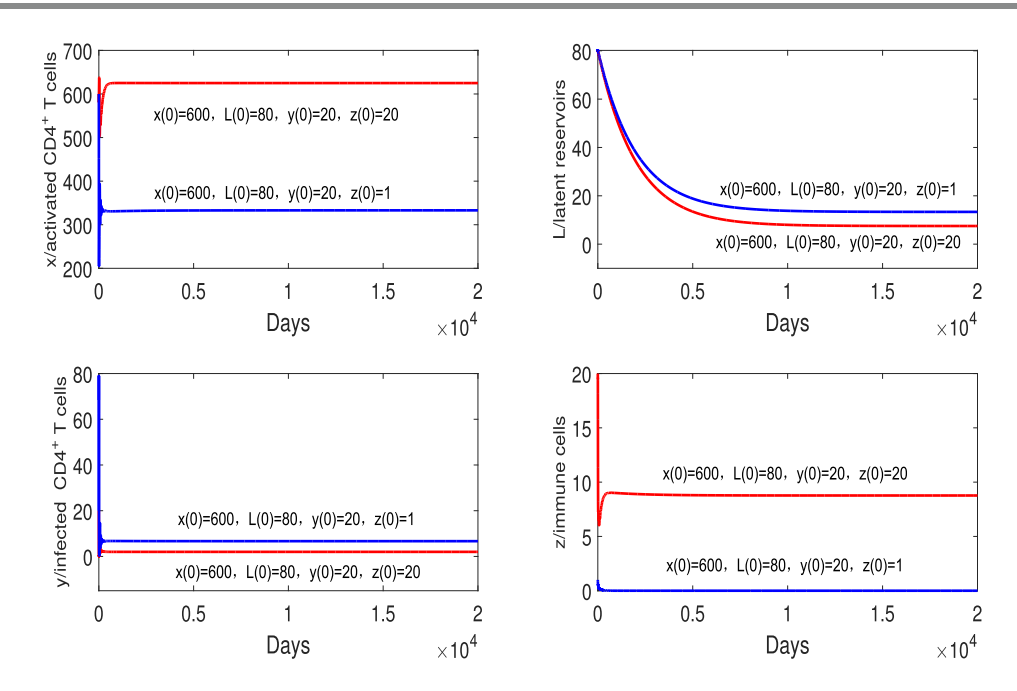


Figure 11. Bistability of system (1.1) with initial values x(0) = 600, L(0) = 80, y(0) = 20, z(0) = 1 (blue) and x(0) = 600, L(0) = 80, y(0) = 20, z(0) = 20 (red). The parameter values are listed in Table 7. (Figure in color online.)

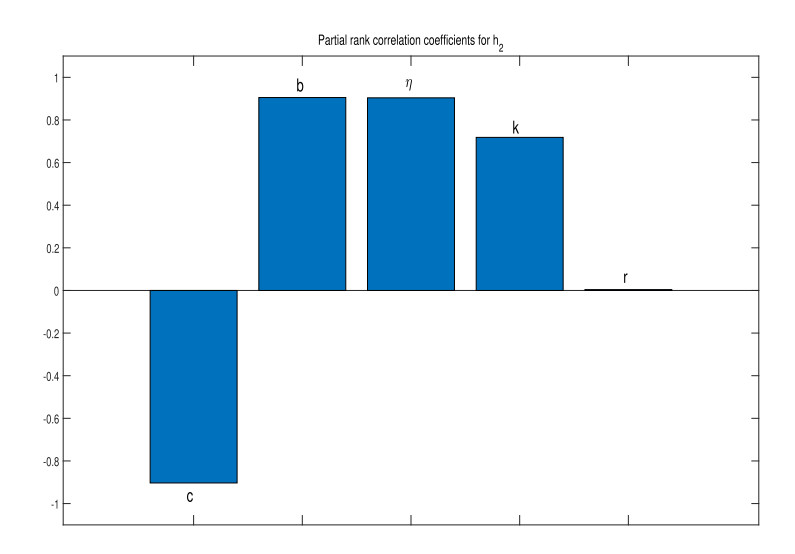


Figure 12. Partial rank correlation coefficients show the dependence of h_2 on each parameter.

Appendix A. Proof of Theorem 2.1.

Proof. According to the fundamental theory of ordinary differential equations, system (1.1), with nonnegative initial conditions, possesses a unique solution. For any nonnegative initial data, let $t_1 > 0$ denote the first time at which $x(t_1) = 0$. The first equation of (1.1) implies that $\dot{x}(t_1) = s > 0$. This implies that x(t) < 0 for $t \in (t_1 - \varepsilon_1, t_1)$, where ε_1 is

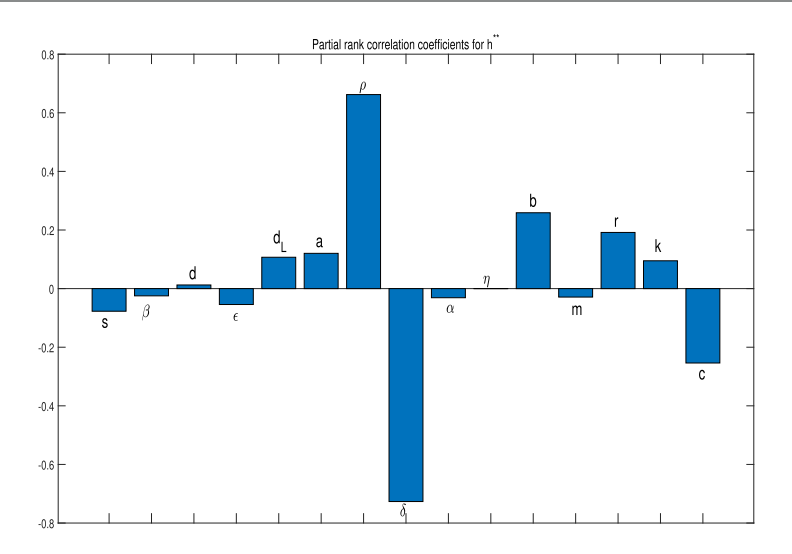


Figure 13. Partial rank correlation coefficients show the dependence of h^{**} on each parameter.

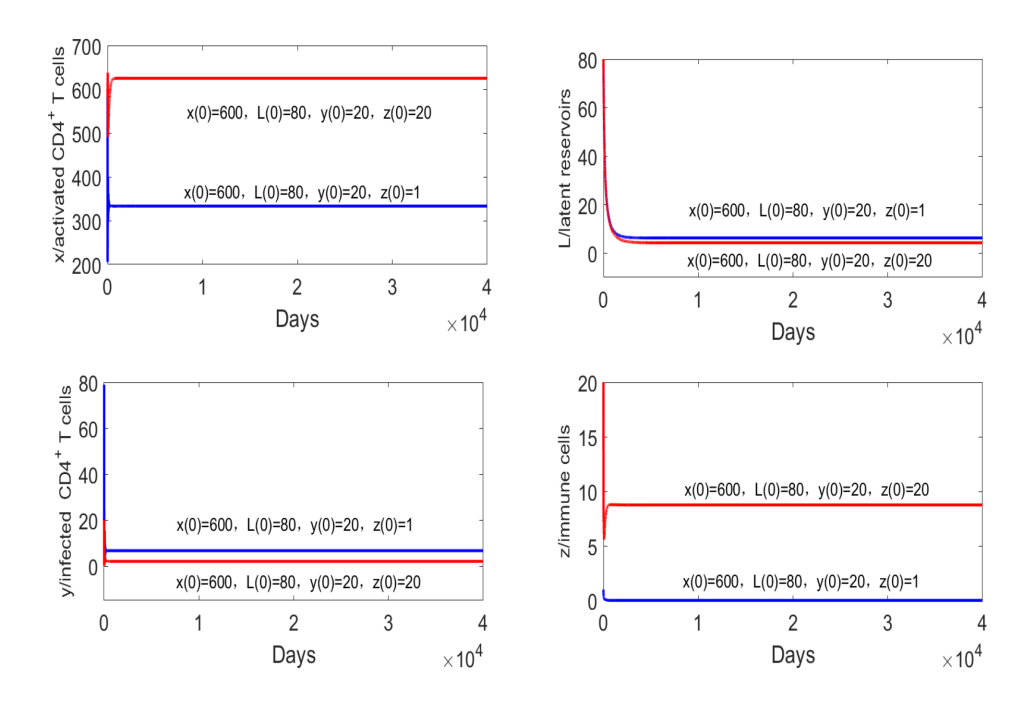


Figure 14. Bistability of system (6.1) with $L_{max} = 50$. The initial values are x(0) = 600, L(0) = 20, y(0) = 20, z(0) = 1 (blue) and x(0) = 600, L(0) = 80, y(0) = 20, z(0) = 20 (red). The parameter values are listed in Table 7. (Figure in color online.)

an arbitrarily small positive constant. However, the aforementioned discussion leads to a contradiction. Hence, it can be concluded that x(t) remains positive. As the last equation of (1.1) has a constant solution z = 0, the fundamental existence and uniqueness theorem establishes that z > 0 for all t > 0.

Suppose that at time $t_2 > 0$, $y(t_2)z(t_2)$ reaches 0 for the first time. Thus, we have

- (i) $L(t_2) = 0, y(t) \ge 0$ for $t \in [0, t_2]$, or
- (ii) $y(t_2) = 0, L(t) \ge 0$ for $t \in [0, t_2]$.

For case (i), because x(t) is positive, it follows from the variation of constants formula that $L(t_2) = L(0) + e^{-\int_0^{t_2} (a + d_L - \hat{\rho}) d\xi} \int_0^{t_2} \alpha_L(1 - \epsilon) \beta_L(\xi) y(\xi) d\xi > 0$, which is in contradiction with $L(t_2) = 0$.

For case (ii), the third equation of system (1.1) implies that $y(t_2) = y(0) + e^{\int_0^{t_2} [(1-\alpha_L)(1-\epsilon)\beta x(\xi)-\delta-pz(\xi)]d\xi} \int_0^{t_2} aL(\xi)d\xi > 0$, which contradicts $y(t_2) = 0$. Thus, L(t) and y(t) are always positive.

Next, we will elaborate on the boundedness of the solutions to system (1.1). Let

$$M(t) = \sigma x(t) + aL(t) + (a + d_L - \rho)y(t) + \frac{pk(a + d_L - \rho)z(t)}{ch},$$

where $\sigma = a\alpha_L + (1 - \alpha_L)(a + d_L - \rho)$. Since all solutions of (1.1) are positive, we have

$$\begin{split} \frac{dM}{dt} &= \sigma \left[s - dx - (1 - \epsilon)\beta xy \right] + a \left[\alpha_L (1 - \epsilon)\beta xy + (\rho - a - d_L)L \right] \\ &+ (a + d_L - \rho) \left[(1 - \alpha_L)(1 - \epsilon)\beta xy + aL - \delta y - pyz \right] \\ &+ \frac{pk(a + d_L - \rho)}{ch} \left(\frac{cyz}{1 + \eta y} \frac{h}{k + ry} - bz \right) \\ &\leq \sigma s - \sigma dx - (a + d_L - \rho)\delta y - \frac{bpk(a + d_L - \rho)z}{ch} \\ &< \sigma s - \nu M \end{split}$$

Here $\nu = \min\{d, \delta, b\}$. Let φ be the solution of

$$\begin{cases} \frac{d\varphi}{dt} = \sigma s - \nu \varphi, \\ \varphi_0 = \sigma x^0 + aL^0 + (a + d_L - \rho)y^0 + \frac{pk(a + d_L - \rho)z^0}{ch}, \end{cases}$$

where x^0, y^0 , and z^0 are initial values of system (1.1) and $\varphi_0 = M_0 > 0$. We then evaluate $\lim_{t\to+\infty}\sup\varphi(t)=\frac{\sigma s}{\nu}$. It follows from the comparison theorem that $M(t)<\varphi(t)$. Thus, x(t), L(t), y(t), and z(t) are bounded.

Appendix B. Proof of Theorem 3.1.

Proof. It is clear that the characteristic equation at the equilibrium $E_0(x_0,0,0,0)$ has two negative roots -d and -b. The other two eigenvalues are solutions of

(B.1)
$$\lambda^2 + a_1\lambda + a_2 = 0,$$

where

$$a_{1} = a + d_{L} - \rho + \delta \left[1 - \frac{(1 - \alpha_{L})(1 - \epsilon)\beta x_{0}}{\delta} \right],$$

$$a_{2} = (a + d_{L} - \rho) - a\beta(1 - \epsilon)[\delta - (1 - \alpha_{L})(1 - \epsilon)\beta x_{0}] - \frac{as\beta\alpha_{L}(1 - \epsilon)}{d}$$

$$= \delta(a + d_{L} - \rho)(1 - R_{0}).$$

It is easy to see that $a_1 > 0$ and $a_2 > 0$ for $R_0 < 1$. Therefore, when $R_0 < 1$, (B.1) has two negative roots, indicating that E_0 is locally stable. On the other hand, when $R_0 > 1$, we have $a_2 < 0$. E_0 is a saddle with dim $W^s(E_0) = 2$ and dim $W^u(E_0) = 1$, and it is hence unstable. This completes the proof of Theorem 3.1.

Appendix C. Proof of Theorem 3.2.

Proof. Define a function

$$V = \frac{1}{2}(x - x_0)^2 + AL + By + \frac{pB}{ch}z,$$

where A and B are positive coefficients to be determined. It is easy to see that V is a positive Lyapunov function. Evaluating the time derivative of V along the solution of system (1.1) yields

$$\begin{split} \dot{V}\|_{(1.1)} &= (x-x_0) \left[s - dx - (1-\epsilon)\beta xy \right] + A \left[\alpha_L (1-\epsilon)\beta xy - (a+d_L-\rho)L \right] \\ &+ B \left[(1-\alpha_L)(1-\epsilon)\beta xy + aL - \delta y - pyz \right] + \frac{pB}{ch} \left(\frac{cyz}{1+\eta y} \frac{h}{k+ry} - bz \right) \\ &= (x-x_0) \left[dx_0 - dx - (1-\epsilon)\beta xy + (1-\epsilon)\beta x_0y - (1-\epsilon)\beta x_0y \right] \\ &+ A\alpha_L (1-\epsilon)\beta xy - A(a+d_L-\rho)L + B(1-\alpha_L)(1-\epsilon)\beta xy \\ &+ BaL - B\delta y - Bpyz + \frac{pB}{ch} \frac{cyz}{1+\eta y} \frac{h}{k+ry} - \frac{pB}{ch} bz \\ &\leq - \left(d + (1-\epsilon)\beta y \right) (x-x_0)^2 - \left[x_0 - A\alpha_L - B(1-\alpha_L) \right] (1-\epsilon)\beta xy \\ &- \left[B\delta - (1-\epsilon)\beta x_0^2 \right] y - \left[A(a+d_L-\rho) - Ba \right] L - \frac{pB}{ch} bz. \end{split}$$

Choosing

$$\begin{split} A &= \frac{x_0}{(1-\alpha_L)\left[\frac{a+d_L-\rho}{a} + \frac{\alpha_L}{1-\alpha_L}\right]}, \\ B &= \frac{A(a+d_L-\rho)}{a}, \end{split}$$

we get

$$x_0 - A\alpha_L - B(1 - \alpha_L) \ge 0,$$

$$B\delta - (1 - \epsilon)\beta x_0^2 \ge 0,$$

$$A(a + d_L - \rho) - Ba \ge 0.$$

Thus, if $R_0 \le 1$, we have $\dot{V}\|_{(1.1)} \le 0$. Since x, L, y, and z are positive, we get $\dot{V}\|_{(1.1)} = 0$ if and only if $(x, L, y, z) = (x_0, 0, 0)$. It thus follows from the classical Krasovskii–LaSalle principle that E_0 is globally asymptotically stable.

Appendix D. Proof of Theorem 3.3.

Proof. The characteristic equation of the linearized system of (1.1) at E_1 is given by

$$(\lambda^3 + b_1 \lambda^2 + b_2 \lambda + b_3) \left[\frac{chy_1}{(1 + \eta y_1)(k + ry_1)} - b \right] = 0,$$

where

$$\begin{split} b_1 &= d + (1 - \epsilon)\beta y_1 + a + d_L - \rho + \frac{a\alpha_L(1 - \epsilon)\beta x_1}{a + d_L - \rho}, \\ b_2 &= d(a + d_L - \rho + \frac{aL_1}{y_1}) + (1 - \epsilon)\beta aL_1 + (1 - \epsilon)\beta y_1(a + d_L - \rho) \\ &\quad + (1 - \epsilon)\beta x_1(1 - \alpha_L)(1 - \epsilon)\beta y_1, \\ b_3 &= a\alpha_L(1 - \epsilon)\beta x_1(1 - \epsilon)\beta y_1 + (a + d_L - \rho)(1 - \epsilon)\beta x_1(1 - a_L)(1 - \epsilon)\beta y_1. \end{split}$$

Furthermore, we have

$$\begin{split} b_1 b_2 - b_3 &= b_2 [d + (1 - \epsilon) \beta y_1] + (a + d_L - \rho) \Bigg[d \left(a + d_L - \rho + \frac{aL_1}{y_1} \right) \\ &+ (1 - \epsilon) \beta aL_1 + (1 - \epsilon) \beta y_1 (a + d_L - \rho) \Bigg] + \big[\frac{a\alpha_L (1 - \epsilon) \beta x_1}{a + d_L - \rho} \big] [d(a + d_L - \rho) + \frac{aL_1}{y_1}) + (1 - \epsilon) \beta aL_1 + (1 - \epsilon) \beta x_1 (1 - \alpha_L) (1 - \epsilon) \beta y_1] \\ &> 0. \end{split}$$

Next, we determine the sign of the eigenvalue. We have

$$\lambda_4 = \frac{chy_1}{(1 + \eta y_1)(k + ry_1)} - b < 0$$

$$\Leftrightarrow \frac{-br\eta y_1^2 + (ch - br - bk\eta)y_1 - bk}{(1 + \eta y_1)(k + ry_1)} < 0$$

$$\Leftrightarrow h < h^{**}.$$

From the Routh–Hurwitz criterion, the assumption $R_0 > 1$, and $0 < h < h^{**}$, we know that the equilibrium E_1 of system (1.1) is locally asymptotically stable. On the other hand, when $h > h^{**}$, E_1 is unstable.

Appendix E. Proof of Theorem 3.4.

Proof. The characteristic equation of the linearized system of (1.1) at any arbitrary positive equilibrium E^* is obtained as

$$\lambda^4 + A_1 \lambda^3 + A_2 \lambda^2 + A_3 \lambda + A_4 = 0,$$

where

$$\begin{split} A_1 &= a + d_L - \rho + d + \beta (1 - \epsilon) y^* + \frac{aL^*}{y^*}, \\ A_2 &= (a + d_L - \rho) \left[d + \beta (1 - \epsilon) y^* \right] + \frac{aL^*}{y^*} \left[d + \beta (1 - \epsilon) y^* \right] \\ &\quad + p y^* z^* \frac{chz^*(k - \eta r y^{*2})}{(1 + \eta y^*)^2 (k + r y^*)^2} + (1 - \alpha_L) (1 - \epsilon) \beta x^* (1 - \epsilon) \beta y^*, \\ A_3 &= \frac{aL^*}{y^*} (a + d_L - \rho) (1 - \epsilon) \beta y^* + (1 - \alpha_L) (1 - \epsilon) \beta x^* (1 - \epsilon) \beta y^* (a + d_L - \rho) \\ &\quad + p y^* z^* \frac{chz^*(k - \eta r y^{*2})}{(1 + \eta y^*)^2 (k + r y^*)^2} \left[a + d_L - \rho + d + \beta (1 - \epsilon) y^* \right], \\ A_4 &= p y^* z^* \frac{chz^*(k - \eta r y^{*2})}{(1 + \eta y^*)^2 (k + r y^*)^2} (a + d_L - \rho) \left[d + \beta (1 - \epsilon) y^* \right]. \end{split}$$

Then we have

$$\begin{split} A_1 A_2 - A_3 &= \frac{aL^*}{y^*} d(a + d_L - \rho) + (\frac{aL^*}{y^*})^2 \left[d + \beta (1 - \epsilon) y^* \right] \\ &+ \frac{aL^*}{y^*} p y^* z^* \frac{chz^* (k - \eta r y^{*2})}{(1 + \eta y^*)^2 (k + r y^*)^2} + \frac{aL^*}{y^*} (1 - \alpha_L) (1 - \epsilon) \beta x^* (1 - \epsilon) \beta y^* \\ &+ \left[a + d_L - \rho + d + \beta (1 - \epsilon) y^* \right] (a + d_L - \rho) \left[d + \beta (1 - \epsilon) y^* \right] \\ &+ \frac{aL^*}{y^*} \left[d + \beta (1 - \epsilon) y^* \right] \left[a + d_L - \rho + d + \beta (1 - \epsilon) y^* \right] \\ &+ (1 - \alpha_L) (1 - \epsilon) \beta x^* (1 - \epsilon) \beta y^* \left[a + d_L - \rho + d + \beta (1 - \epsilon) y^* \right]. \end{split}$$

(i) For equilibrium E_{-}^{*} , we have

$$k - \eta r y_{-}^{*2} > 0 \Leftrightarrow h > h_2.$$

If $h > h_2$, then $A_4 > 0$. Clearly, $A_i > 0$, i = 1, 2, 3 and $A_1A_2 - A_3 > 0$. If $A_3(A_1A_2 - A_3) - A_1^2A_4 > 0$, from the Routh-Hurwitz criterion, we know that the positive equilibrium E_-^* is a stable node.

(ii) For equilibrium E_+^* , we have

(E.1)
$$k - \eta r y_+^{*2} < 0 \Leftrightarrow 2b\sqrt{rk\eta} - B < \sqrt{B^2 - 4b^2 rk\eta}.$$

For $h_2 < h < h^{**}$, (E.1) holds true. Thus, equilibrium E_+^* is unstable.

REFERENCES

- [1] C. Bartholdy, J. Christensen, D. Wodarz, and A. Thomsen, Persistent virus infection despite chronic cytotoxic T-lymphocyte activation in gamma interferon-deficient mice infection with lymphocytic choriomeningitis virus, J. Virol., 74 (2000), pp. 10304–10311.
- [2] S. Blower and H. Dowlatabadi, Sensitivity and uncertainty analysis of complex models of disease transmission: An HIV model, as an example, Int. Stat. Rev., 2 (1994), pp. 229–243.
- [3] R. D. Boer and A. Perelson, Target cell limited and immune control models of HIV infection: A comparison, J. Theoret. Biol., 190 (1998), pp. 201–214.
- [4] S. Bonhoeffer, M. Rembiszewski, G. Ortiz, and D. Nixon, Risks and benefits of structured antiretroviral drug therapy interruptions in HIV-1 infection, AIDS, 14 (2000), pp. 2313–2322.
- [5] P. Borrow, H. Lewicki, X. Wei, S. Horwitz, N. Peffer, H. Meyers, J. Nelson, J. Gairin, B. Hahn, M. Oldstone, and G. Shaw, Antiviral pressure exerted by HIV-1-specific cytotoxic T lymphocytes (CTLs) during primary infection demonstrated by rapid selection of CTL escape virus, Nat. Med., 3 (1997), pp. 205–211.
- [6] C. Castillo-Chavez and B. Song, Dynamical models of tuberculosis and their applications, Math. Biosci. Eng., 1 (2004), pp. 361–404.
- [7] J. Conway and A. Perelson, *Post-treatment control of HIV infection*, Proc. Natl. Acad. Sci. USA, 112 (2015), pp. 5467–5472.
- [8] J. COURET AND T. L. CHANG, Reactive oxygen species in HIV infection, EC Microbiol., 3 (2016), pp. 597–604.
- [9] S. DEBROY, B. BOLKER, AND M. MARTCHEVA, Bistability and long-term cure in a within-host of Hepatitis C, J. Biol. Syst., 19 (2011), pp. 533-550.
- [10] R. V. GAALEN AND L. WAHL, Reconciling conflicting clinical studies of antioxidant supplementation as HIV therapy: A mathematical approach, BMC Public Health, 9 (2009), S12.

- [11] P. GOULDER, R. PHILLIPS, R. COLBERT, S. MCADAMA, M. OGGA, P. GIANGRANDEC, G. LUZZID, B. MORGANE, A. EDWARDSE, A. McMichaela, and S. Rowland-Jonesa, Late escape from an immunodominant cytotoxic T-lymphocute response associated with progression to aids, Nat. Med., 3 (1997), pp. 212–217.
- [12] K. Gulow, M. Kaminski, K. Darvas, D. Suss, M. Li-Weber, and P. H. Krammer, HIV-1 transactivator of transcription substitutes for oxidative signaling in activation-induced T cell death, J. Immunol., 174 (2005), pp. 5249–5260.
- [13] T. Guo, Z. Qiu, and L. Rong, Analysis of an HIV model with immune responses and cell-to-cell transmission, Bull. Malays. Math. Sci. Soc., 43 (2020), pp. 581–607.
- [14] S. Hoshino, M. Konishi, M. Mori, M. Shimura, C. Nishitani, Y. Kuroki, Y. Koyanagi, S. Kano, H. Itabe, and Y. Ishizaka, HIV-1 Vpr induces TLR4/MyD88-mediated IL-6 production and reactivates viral production from latency, J. Leukocyte Biol., 87 (2010), pp. 1133–1143.
- [15] A. V. IVANOV, V. T. VALUEV-ELLISTON, O. N. IVANOVA, S. N. KOCHETKOV, E. S. STARODUBOVA, B. BARTOSCH, AND M. G. ISAGULIANTS, Oxidative stress during HIV infection: Mechanisms and consequences, Oxidative Med. Cell. Longev., 2016 (2016), 8910396.
- [16] S. IWAMI, T. MIURA, S. NAKAOKA, AND Y. TAKEUCHI, Immune impairment in HIV infection: Existence of risky and immunodeficiency thresholds, J. Theoret. Biol., 260 (2009), pp. 490–501.
- [17] S. IWAMI, S. NAKAOKA, Y. TAKEUCHI, AND T. MIURA, Immune impairment thresholds in HIV infection, Immunol. Lett., 123 (2009), pp. 149–154.
- [18] P. Johnson, B. Kochin, M. McAfee, I. Stromnes, R. Regoes, R. Ahmed, J. Blattman, and R. Antia, Vaccination alters the balance between protective immunity, exhaustion, escape, and death in chronic infections, J. Virol., 85 (2011), pp. 5565–5570.
- [19] D. KAUFMANN AND B. WALKER, PD-1 and CTLA-4 inhibitory co-signaling pathways in HIV infection and the potential for therapeutic intervention, J. Immunol., 182 (2009), pp. 5891–5897.
- [20] A. KHAITAN AND D. UNUTMAZ, Revisiting immune exhaustion during HIV infection, Curr. HIV/AIDS Rep., 8 (2011), pp. 4–11.
- [21] H. Kim and A. Perelson, Viral and latent reservoir persistence in HIV-1C infected patients on therapy, PLoS Comput. Biol., 2 (2006), e135.
- [22] N. Komarova, E. Barnes, P. Klenerman, and D. Wodarz, Boosting immunity by antiviral drug therapy: A simple relationship among timing, efficacy, and success, Proc. Natl. Acad. Sci. USA, 100 (2003), pp. 1855–1860.
- [23] S. Marino, I. Hogue, C. Ray, and D. Kirschner, A methodology for performing global uncertainty and sensitivity analysis in systems biology, J. Theoret. Biol., 254 (2008), pp. 178–196.
- [24] B. J. NATH, K. DEHINGIA, K. SADRI, H. K. SARMAH, K. HOSSEINI, AND C. PARK, Optimal control of combined antiretroviral therapies in an HIV infection model with cure rate and fusion effect, Int. J. Biomath., 16 (2023), 2250062.
- [25] M. NOWAK AND C. BANGHAM, Population dynamics of immune response to persistent viruses, Science, 272 (1996), pp. 74–79.
- [26] M. NOWAK, R. MAY, R. PHILLIPS, S. ROELAND-JONES, D. LALLOO, S. MCADAM, P. KLENERMAN, B. KÖPPE, K. SIGMUND, C. BANGHAM, AND A. MCMICHAEL, Antigenic oscillations and shifting immunodominance in HIV-1 infections, Nature, 375 (1995), pp. 606-611.
- [27] D. Persaud, H. Gay, C. Ziemniak, Y. Chen, M. Piatak, T. Chun, M. Strain., D. Richman, and K. Luzuriaga, Absence of detectable HIV-1 viremia after treatment cessation in an infant, N. Engl. J. Med., 369 (2013), pp. 1828–1835.
- [28] R. Phillips, S. Rowland-Jones, D. Nixon, F. Gotch, J. Edwards, A. Ogunlesi, J. Elvin, J. Rothbard, C. Bangham, C. Rizza, and A. McMichael, *Human immunodeficiency virus genetic variation that can escape cytotoxic T cell recognition*, Nature, 354 (1991), pp. 453–459.
- [29] D. PRICE, P. GOULDER, P. KLENERMAN, A. SEWELL, P. EASTERBROOK, M. TROOP, C. BANGHAM, AND R. PHILLIPS, *Positive selection of HIV-1 cytotoxic T lymphocyte escape variants during primary infection*, Proc. Natl. Acad. Sci USA, 94 (1997), pp. 1890–1895.
- [30] A. Pugliese and A. Gandolfi, A simple model of pathogen-immune dynamics including specific and non-specific immunity, Math. Biosci., 214 (2008), pp. 73–80.
- [31] R. Regoes, D. Wodarz, and M. Nowak, Virus dynamics: The effect of target cell limitation and immune responses on virus evolution, J. Theoret. Biol., 191 (1998), pp. 451–462.

- [32] A. C. Roc, B. M. Ances, S. Chawla, M. Korczykowski, R. L. Wolf, D. L. Kolson, J. A. Detre, and H. Poptani, Detection of human immunodeficiency virus-induced inflammation and oxidative stress in lenticular nuclei with magnetic resonance spectroscopy despite antiretroviral therapy, Arch. Neurol., 64 (2007), pp. 1249–1257.
- [33] L. RONG AND A. PERELSON, Asymmetric division of activated latently infected cells may explain the decay kinetics of the HIV-1 latent reservoir and intermittent viral blips, Math. Biosci., 217 (2009), pp. 77–87.
- [34] L. RONG AND A. PERELSON, Modeling HIV persistence, the latent reservoir, and viral blips, J. Theoret. Biol., 260 (2009), pp. 308–331.
- [35] S. Salmen and L. Berrueta, Immune modulators of HIV infection: The role of reactive oxygen species, J. Clin. Cell Immunol., 3 (2012), 2.
- [36] C. SÁNCHEZ-POZO, J. RODRIGUEZ-BANO, A. DOMÍNGUEZ-CASTELLANO, M. MUNIAIN, R. GOBERNA, AND V. SÁNCHEZ-MARGALET, Leptin stimulates the oxidative burst in control monocytes but attenuates the oxidative burst in monocytes from HIV-infected patients, Clin. Exp. Immunol., 134 (2003), pp. 464–469.
- [37] S. WANG AND L. RONG, Stochastic population switch may explain the latent reservoir stability and intermittent viral blips in HIV patients on suppressive therapy, J. Theoret. Biol., 360 (2014), pp. 137–148.
- [38] S. WANG AND F. Xu, Thresholds and bistability in virus-immune dynamics, Appl. Math. Lett., 78 (2018), pp. 105–111.
- [39] Z. Wang and X. Liu, A chronic viral infection model with immune impairment, J. Theoret. Biol., 249 (2007), pp. 532–542.
- [40] D. WODARZ, J. CHRISTENSEN, AND A. THOMSEN, The importance of lytic and nonlytic immune response in viral infections, Trends Immunol., 23 (2002), pp. 194–200.
- [41] Y. XIAO, S. TANG, Y. ZHOU, R. SMITH, J. WU, AND N. WANG, Predicting the HIV/AIDS epidemic and measuring the effect of mobility in mainland China, J. Theoret. Biol., 317 (2013), pp. 271–285.
- [42] Y. Xu, Y. Yang, F. Meng, and P. Yu, Modeling and analysis of recurrent autoimmune disease, Nonlinear Anal. Real, 54 (2020), pp. 103–109.
- [43] H. C. Yang, S. Xing, L. Shan, K. O'Connell, J. Dinoso, A. Shen, Y. Zhou, C. K. Shrum, Y. Han, J. O. Liu, H. Zhang, J. B. Margolick, and R. F. Siliciano, Small-molecule screening using a human primary cell model of HIV latency identifies compounds that reverse latency without cellular activation, J. Clin. Invest., 119 (2009), pp. 3473–3486.
- [44] J. Zhang, W. Hao, and Z. Jin, Dynamic analysis of an HIV/AIDS treatment model incorporating MSM, Int. J. Biomath., 15 (2022), 2250029.
- [45] W. Zhang, L.M. Wahl, and P. Yu, Conditions for transient viremia in deterministic in-host models: Viral blips need no exogenous trigger, SIAM J. Appl. Math., 73 (2013), pp. 853–881, https://doi.org/10.1137/120884535.
- [46] W. Zhang, L. M. Wahl, and P. Yu, Viral blips may not need a trigger: How transient viremia can arise in deterministic in-host models, SIAM Rev., 56 (2014), pp. 127–155, https://doi.org/10.1137/130937421.